To Appear, IEEE Int. Conf. on Robotics and Biomimetics (ROBIO), Dec. 3-7, Qingdao, China, 2016.

Cooperative Multi-Robot Information Acquisition based on Distributed Robust Model Predictive Control *

Shuhei Emoto, Ilge Akkaya, *Member IEEE*, and Edward A. Lee, *Fellow IEEE*

***Abstract*— In this paper, we propose a distributed multi-robot control system working in dynamic and uncertain environments. Robust model predictive control (robust MPC) enables robots to deal with uncertainties. However, the performance of the robust MPC is dependent on the amount of uncertainty that derives from noisy measurements, communication disturbance, etc. The proposed system includes multiple observation robots that gather information cooperatively as well as a main robot controlled by robust MPC. Therefore, the system works for not only treating the uncertainty but also decreasing it. A simulation result of a collision avoidance shows that the information acquisition by the observation robots enables the main robot to move efficiently and arrive at the goal faster than a case without the observation robots. We also focus on a problem that a large number of observation robots will increase the frequency of inter-robot collision avoidances, and thus negatively affect to the performance of the main robot. Simulation results under various conditions on a disturbance level and a measurement range of sensors clarifies an adequate number of observation robots as well as the design guideline about sensors and networks.**

I. Introduction

Robotic applications such as transportation, surveillance, and disaster response have received a lot of attention in recent years (Fig. 1). In these applications, robotic vehicles commonly work in dynamic environments surrounded by potential obstacles including other robots, human workers, unknown rubble, etc. Furthermore, when robots work in unstructured environments such as construction sites or disaster sites, a large set of uncertainties (e.g. noisy measurements, sensing error, communication disturbance, etc.) influences the control mechanism of robots.

Model Predictive Control (MPC) is a popular control technique to deal with constrained time-variant problems including collision avoidance. The MPC approach predicts future states of robots and objects in the given environment and optimizes the control inputs for such robots so that any subsequent predicted conditions will turn out to be most optimal. In order to tackle uncertainties in addition to dynamic constraints, Robust MPC [1] and Stochastic MPC [2] are

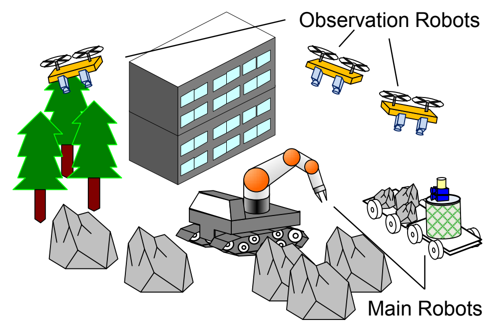

Figure 1. Robotic application in outdoor environment

proposed. The robust MPC framework predicts reachability sets of the future states and finds the control inputs that make these sets satisfy all of the given constraints even in the presence of some prediction errors. Although robust MPC enables robots to work in considerably uncertain environments, the performance of such robots would still heavily depend on the level of uncertainty, mainly due to the conservative nature of the robust MPC approach. This uncertainty is intrinsic to the relative topology of the robots and the obstacles, and in general, cannot be compensated for with computational methods alone. In order to optimize the performance of the robust MPC, it would be necessary to mitigate the level of uncertainty by cooperative exploration.

There is extensive work on an information-theoretic control strategy for minimizing the uncertainties using multiple robots equipped with sensors. Hoffman and Tomlin [3] developed a control method which maximizes mutual information between the sensors and the state of a target in the environment. The mutual information is computed using a particle filter representation of the posterior probability distribution of the target state. Charrow et al. [4] propose approximated representation of mutual information in order to reduce the computational complexity.

In this paper, we study a multi-robot system that consists of cooperative observation robots as well as a main robot operated by higher-level controller. Since all robots are controlled by the robust MPC, they can treat uncertainties properly. In addition, the proposed system has the ability to carry out information acquisition using the observation robots which have the mutual information based control objective [3], [4]. Our previous study demonstrated that information gathering behaviors of the observation robots can positively contribute to the control task carried out by the main robot [5]. This paper evaluates the performance of the main robot under various conditions on a disturbance level and a measurement range of sensors, focusing on the positive and negative impact of the number of the observation robots. Simulation results

* This work was supported in part by the Berkeley Ubiquitous SwarmLab and the TerraSwarm Research Center, one of six centers administered by the STARnet phase of the Focus Center Research Program (FCRP) a Semiconductor Research Corporation program sponsored by MARCO and DARPA.

S. Emoto is with the IHI Corporation, Yokohama, Kanagawa 235-8501, Japan (phone: +81-45-759-2865; fax: +81-45-759-2209; e-mail: syuuhei_emoto@ihi.co.jp).

I. Akkaya and E. A. Lee are with the Electrical Engineering and Computer Sciences Department, University of California at Berkeley, Berkeley, CA 94720 USA (e-mail: ilgea@eecs.berkeley.edu; eal@eecs.berkeley.edu).

clarify the adequate number of observation robots in the proposed system as well providing a design guideline about sensors and networks. Our modeling and simulation approach can be also applicable to several areas in which multi-robot systems carry out a hybrid of multi-objective control patterns, for which rapid prototyping and on-line repurposing of control objectives become crucial.

II. Framework of Multi-robot System

A. Main Framework

One example in the aforementioned applications is a disaster response scenario, in which a team of robotic vehicles is to carry out removal of rubble and search and rescue missions, as depicted in Fig. 1. In this scenario, manipulators and transporters, which have specific duties, are labeled as the "Main robots". Aside from these, we consider a team of "Observation robots," which cooperatively observe the environment. The controller for each robot consists of "Estimator" and "Optimizer" as depicted in Fig. 2. The main robots and the observation robots are subject to the same control flow, but they use robot-specific control objective functions in the optimizer.

B. Measurement and Estimation

Robots can be equipped with one or many sensors such as cameras, lasers, and ultra-sonic sensors. In the proposed system, the measurements of these sensors are broadcast among all robots. The estimator receives measurements from all other robots as well as on-board sensors and performs target state estimation using an Unscented Kalman Filtering (UKF).

In this paper, we consider a collision avoidance scenario shown in Fig. 3 that would happen frequently while the main robot performs transportation tasks. In that scenario, a robot equipped with a range-only sensor is to estimate the position and velocity of a moving obstacle and try to move from a starting point in 2-D space to a final target point, respectively chosen to be (30, 0) and (0, 0), keeping the distance to the obstacle larger than 2 m. For the target state estimation, we use the state-space model given by

$$X_t = \begin{bmatrix} Po_t & Vo_t \end{bmatrix}^T ,$$
$$X_{t+\Delta t} = \begin{bmatrix} 1 & \Delta t \\ 0 & 1 \end{bmatrix} \cdot \begin{bmatrix} Po_t \\ Vo_t \end{bmatrix} + \omega_t , \tag{1}$$
$$z_t = \left\| Po_t - Pr_t \right\|_2 + \eta_t ,$$

where Po_t, Vo_t are the 2-D position and velocity of the obstacle, respectively, and Pr_t is a position of the robot given by its localizer (e.g. GPS, Dead reckoning). ω_t and η_t are assumptions of process noise and measurement noise, respectively. Δt is a time interval of measurement and control.

C. Distributed Robust MPC for the Main Robot

The control input to the main robot is acceleration input, computed according to distributed robust MPC [6] depicted in Fig. 4. The rationale of distributed MPC is that each robot transmits to the others a planned reachability set of trajectory

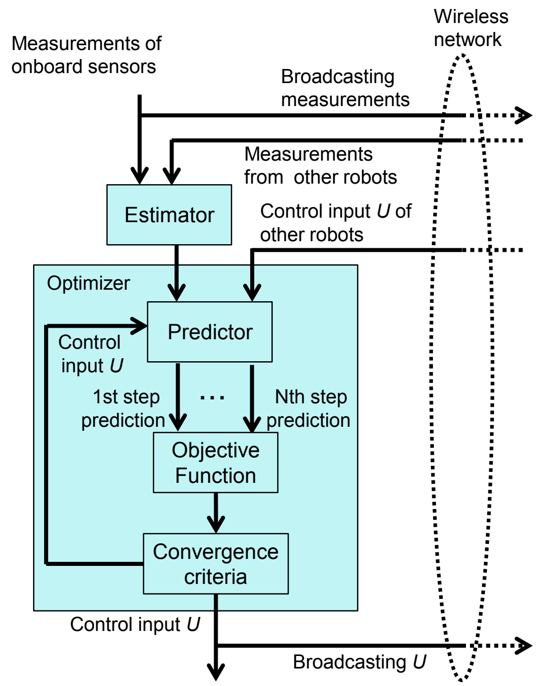

Figure 2. Control flow of each robot

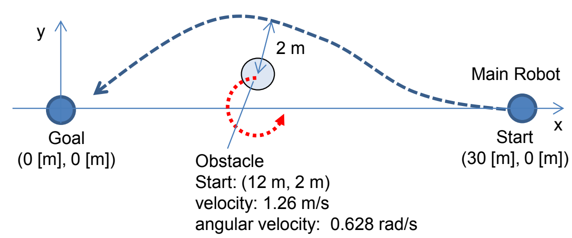

Figure 3. Scheme of the collision avoidance scenario

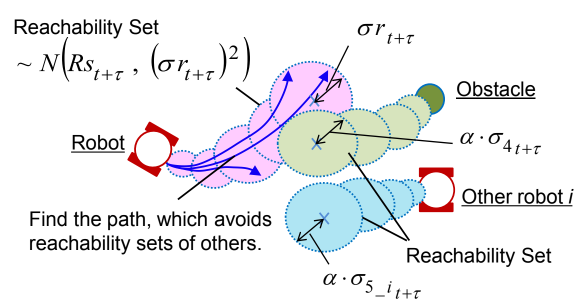

Figure 4. Scheme of the distributed robust MPC

over the prediction horizon and guarantees that its actual trajectory lies in the reachability set. In the proposed system, planned control inputs U over the prediction horizon are broadcasted as shown in Fig. 2 so that each robot can predict the reachability sets of other robots using received messages.

The reachability sets of all robots and the obstacle are determined as a normal distribution at each time step as shown in Fig. 4. Using these predicted states, the acceleration input of the main robot is obtained by solving an optimization problem given by

$$\min_{U_{t+1}\cdots U_{t+s}} \sum_{s=1}^{N} f_0 \qquad \left(f_0 = \left|Pr_{t+\tau}\right|^2,\ \tau = s\cdot\Delta t\right), \tag{2}$$

subject to:

$$\begin{bmatrix} Pr_{t+\Delta t} \\ V_{t+\Delta t} \end{bmatrix} = \begin{bmatrix} 1 & \Delta t \\ 0 & 1 \end{bmatrix} \cdot \begin{bmatrix} Pr_t \\ V_t \end{bmatrix} + \begin{bmatrix} 0 \\ \Delta t \end{bmatrix} \cdot U_t,$$

$$\begin{aligned} f_1 &\leq -\alpha\cdot\sigma_{1t+\tau} && \left(f_1 = \left|V_{t+\tau}\right|^2 - Vmax^2\right), \\ f_2 &\leq -\alpha\cdot\sigma_{2t+\tau} && \left(f_2 = \left|U_{t+\tau}\right|^2 - Amax^2\right), \\ f_3 &\leq -\alpha\cdot\sigma_{3t+\tau} && \left(f_3 = \left\|Rs_{t+\tau} - Pr_{t+\tau}\right\|_2 - \sigma r_{t+\tau}\right), \\ f_4 &\leq -\alpha\cdot\sigma_{4t+\tau} && \left(f_4 = Dmin - \left\|Po_{t+\tau} - Pr_{t+\tau}\right\|_2\right), \\ f_{5\_i} &\leq -\alpha\cdot\sigma_{5\_i_{t+\tau}} && \left(f_{5\_i} = Dmin - \left\|Roi_{t+\tau} - Pr_{t+\tau}\right\|_2\right), \end{aligned}$$

$(i = 1,\ \cdots,\ n \quad n$: the number of the observation robots)

where V_t and U_t are the velocity and the acceleration of the main robot, respectively. Rs_t is a planned trajectory (future position) of the main robot calculated using the control input calculated at previous time step $\left(U_t,\cdots,U_{t+s-1}\right)$. Roi_t is predicted trajectory of the observation robot i calculated using the control input received from robot i. Note that f_{5_i} is defined for each observation robot. In this paper, a set of f_{5_i}, $\{i = 1,\cdots,n\}$, is denoted by f_5.

The equality constraint in (2) is a dynamics model of an omnidirectional mobile robot. Since the future states of the main robot ($Pr_{t+\tau}, V_{t+\tau}$) obey the dynamics model, $f_0 \sim f_5$ are functions of optimization variables $U_{t+1},\cdots,U_{t+s}$. f_0 is the squared Euclidean distance from the robot to the goal. $f_1 \sim f_5$ are inequality constraints that are required to be satisfied. f_1 and f_2 are the constraints on the velocity and acceleration of the main robot, respectively. *Vmax* is the maximum velocity, and *Amax* is the maximum acceleration, are chosen in accordance with the hardware configuration of the robot. f_3 makes the actual trajectory of the main robot lie in the planned reachability set. $\sigma r_{t+\tau}$ is a radius of the reachability set at time $t+\tau$ calculated by

$$\sigma r_{t+\tau} = \sigma r_0 + \beta\cdot\tau, \tag{3}$$

where σr_0 and β are a predetermined parameters (initial radius and an additive margin). f_4 and f_5 are collision avoidance constraints. For example, when the robot is within a distance *Dmin* to the obstacle, f_4 is positive. Current position of the obstacle Po_t is provided by the estimator at each time step. *Dmin* is a predetermined safety margin on distance to the obstacles.

For the purpose of treating the uncertainty properly, all constraints in (2) are enlarged by given margins $\alpha\cdot\sigma_m$, where $\sigma_m, \{m = 1,\cdots,5\_1,\cdots,5\_n\}$, are standard deviations of the constraint functions f_m. $\sigma_{4t+\tau}$ and $\sigma_{5\_i_{t+\tau}}$ are calculated by

$$\begin{aligned} \sigma_{4t+\tau} &= \sqrt{\left(\frac{\partial f_4}{\partial Po_{t+\tau}}\right)\cdot C_{t+\tau}\cdot\left(\frac{\partial f_4}{\partial Po_{t+\tau}}\right)^T}, \\ \sigma_{5\_i_{t+\tau}} &= \sigma r_{t+\tau} + \beta\cdot di, \end{aligned} \tag{4}$$

where $C_{t+\tau}$ is a covariance matrix of $Po_{t+\tau}$, which can be calculated using current covariance C_t given by UKF, and di is the number of elapsed steps since the latest message of robot i was received. If the obstacle's position Po_t is unknown, then σ_{4t} is large so that the constraint f_4 is tightened. Similarly, if the packet loss of communication occurs frequently, $\sigma_{5\_i_t}$ is large. As illustrated in Fig. 4, σ_{4t} and $\sigma_{5\_i_t}$ represent radii of the reachability sets of the obstacle and the other robots, respectively. Therefore, the main robot will move away from the others proportionally to the scaling factor α. In this paper, $\sigma_{1t+\tau} \sim \sigma_{3t+\tau}$ are set to zero at all times, assuming that $f_1 \sim f_3$ don't include any uncertain variables.

Optimization problem (2) can be solved using general constrained optimization theory. Specifically, we use the interior point barrier-method [7] to solve it.

D. Optimal Control for the Observation Robots

Unlike the case for the main robot, the control objective of the observation robots is not set to be a pursuit goal. The objective instead is to provide as much information as possible about the unknown environment to the main robots by utilizing their on-board sensors and dynamic capabilities (Fig. 5). For the control of observation robots, we use (5) as the objective function instead of (2).

$$\min_{U_{t+1}\cdots U_{t+s}} \left[-I_{t+N\cdot\Delta t} + \gamma\cdot\sum_{s=1}^{N} f_6\right] \tag{5}$$

$$I_t \approx -\sum_{i=1}^{M} w_{t,i}\cdot\log\sum_{j=1}^{M} w_{t,j}\cdot PDF\left(z_{t,i}; z_{t,j}, \eta_t\right)$$

(M: the number of sigma points of UKF)

$$f_6 = \max\left(0, \left\|Po_{t+\tau} - Pr_{t+\tau}\right\|_2 - Dmax\right)$$

subject to the same constraints in (2). I_t is the approximated mutual information between the estimated state of the obstacle and the future measurement of the observation robots described in [4]. PDF is a conditional probability density function. $z_{t,i}$ and $z_{t,j}$ are the prediction of measurements if the robot measures the sigma point i and j, respectively, and η_t is the assumption of measurement noise in (1). More details about information gathering theory using mutual information are described in [3], [4]. f_6 is a soft constraint on the distance to the measurement target. If a distance to the obstacle is more than *Dmax*, f_6 is positive so that the observation robot likely moves closer to the obstacle. γ is a predetermined penalty parameter. *Dmax* is chosen in accordance with the measurement range of the sensor on board the observation robot.

Using the objective function given by (5), observation robots can maximize the mutual information while keeping the distance to the obstacle. As shown in Fig. 5, the behavior of the observation robot minimizes the expected future uncertainty of the obstacle's position estimate.

III. Evaluation of The Multi-robot System

A. Experimental Setup

In order to analyze the effect of the observation robots, the proposed system needs to be evaluated under dynamic and uncertain environments. In this paper, we use Ptolemy II [8], the modeling and simulation environment, to build a test environment in which various disturbances such as sensor noise, sensor errors, and communication errors are simulated. Ptolemy II is a framework for building and simulating actor-oriented models of heterogeneous systems. Furthermore, Ptolemy II offers aspect-oriented modeling environment that enables us to build disturbance models [9] as well as actor libraries for machine learning and optimization tools [10]. In this paper, we build a disturbance model in which the sensor error and the communication error occur with a fixed probability determined as "Disturbance level".

The simulation conditions are summarized in Table I. In this paper, each condition is simulated 100 times and the amount of time required by the main robot to reach the goal is evaluated as a performance indicator. We focus on the performance of the main robot under various conditions on the number of the observation robots, the measurement range and the disturbance level. If the measurement range is short, the observation robots have to be close to measurement target in order to continuously measure it. Consequently, observation robots tend to be deployed in the path of the main robot, forcing the main robot to travel farther in order to avoid the observation robots. The sensor errors and communication errors enlarge the size of the reachability sets, resulting in the decrease of the performance of the main robot. By increasing the number of the observation robots, information about the obstacle would be gathered more effectively. On the other hand, since the observation robots themselves are potential obstacles, too many robots would decrease the performance of the main robot. Simulation results of these conditions can provide an adequate number of the observation robots as well as the design guideline about sensors and networks.

Common parameter settings are summarized in Tables II and III. Even though the obstacle is moving in a circular orbit with constant speed, this is unknown to the robots. The robots estimate the obstacle's position and velocity with linear uniform motion model in (1). To simulate a range-only measurement sensor, the position of the obstacle is calculated with additive Gaussian noise η_t at each time step. σb is set as a large value so that the uncertainty of the obstacle will be an ellipse as illustrated in Fig. 5.

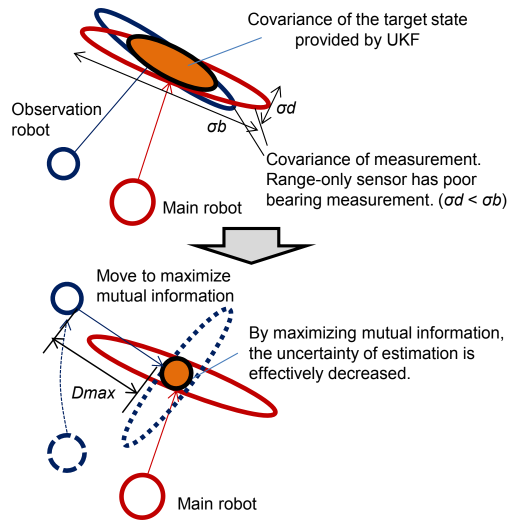

Figure 5. Scheme of the mutual information based control

TABLE I. Simulation Conditions

Simulation Parameter	Value
Measurement range	*Dmax* = 5m, 10m, 15m, 30m
Disturbance level [a]	(0%, 0%), (25%, 25%), (50%, 50%)
No. of the observation robots	0, 1, 2, 3, 4

a. Disturbance level = (probability of packet loss %, probability of failure to measure %)

TABLE II. Parameter Settings for Estimation

Simulation Parameter	Value
Process noise in obstacle's state-space model	$\omega_t \sim N\left((0,0), \begin{pmatrix} Qp & 0 \\ 0 & Qv \end{pmatrix}\right)$, $Qp = \begin{pmatrix} 0.002 & 0 \\ 0 & 0.002 \end{pmatrix}, Qv = \begin{pmatrix} 0.004 & 0 \\ 0 & 0.004 \end{pmatrix}$
Measurement noise	$\eta_t \sim N\left((0,0), \begin{pmatrix} \sigma d^2 & 0 \\ 0 & \sigma b^2 \end{pmatrix}\right)$, $\sigma d = 0.2$ m, $\sigma b = 2$ m

TABLE III. Parameter Settings for Simulation Scenarios

Simulation Parameter	Value
Obstacle's dynamics	Circular Motion Start: (x, y) = (12 m, 2m) Velocity: 1.26 m/s Angular velocity: 0.628 rad/s
Constraints on the control of robots	
Maximum velocity	Main robot: *Vmax* = 8/m/s Observation robot: *Vmax* = 16 m/s
Maximum acceleration	Main robot: *Amax* = 8/m/s^2 Observation robot: *Amax* = 16 m/s^2
Minimum distance to the obstacle and other robots	*Dmin* = 2 m
Size of reachability set	$\alpha = 2$, $\sigma r_0 = 0.2$m, $\beta = 0.4$ m
Penalty parameter of f_6	$\gamma = 0.001$
Time interval	$\Delta t = 0.1$ [s]
Prediction time horizon	$N = 10$ steps (= 1.0 s)

B. Simulation Results

The trajectories of first 10 cases in cases of $Dmax$ = 30m are illustrated in Fig. 6. Average times for the main robot to move to goal are shown in Fig. 7. As shown in Fig. 6, the main robot in every case can safely avoid the obstacle. Comparing Fig. 6(a) and Fig. 6(b), we notice that the trajectories of the main robot with at least one observation robot are shorter than those of the single robot. As shown in Fig. 8, separate trajectories of the observation robots would allow for obstacle observation from different locations. As a result, the obstacle's position is estimated with a high degree of accuracy, in other words, the uncertainty of the obstacle's position estimate is reduced. This could directly lead to a form of constraint relaxation on the main robot, and in turn, allows the main robot to follow a less conservative yet safe trajectory around the obstacle. Consequently, the results in cases with at least one observation robot were better than the condition without the observation robot (See Fig. 7(a), average times in case with the observation robots were shorter than W/O obs. robot).

As shown in Fig. 7, an increase of the disturbance level has a negative effect over all conditions. Because the disturbances enlarge the reachability sets, the main robot needed to be more conservative under higher levels of disturbance. Comparing among 50% of the disturbance level in Fig. 7(a), we realize that the case with 3 observation robots achieved the best performance, while the case with 2 observation robots was the best in 0% and 25% of the disturbance level. These results imply that a system with the large number of observation robots has redundancies of sensing and communication so that the system is robust over the disturbances.

Focusing on the case of 4 observation robots, we realize that the average times were longer than the case with 2 or 3 observation robots in almost all cases. These performance degradations are caused by collision avoidance behaviors frequently occurred between the main robot and the observation robots. For example, as shown in Fig. 6(d), the main robot of 9th trial traveled the longest way because it needed to avoid the observation robot 2 at the beginning of the test (Fig. 8). These results indicate that the system with 3 observation robots has enough redundancy to tackle with the disturbances inserted in this examination. Therefore, the system with 4 or more robots wouldn't have advantages, because too many observation robots frequently force collision avoidance behaviors of the main robot.

The collision avoidance between robots tends to take place in the case of short measurement range. As shown in Fig. 7(b) ~ (d), the performance of the main robot deteriorates as more observation robots are added to the system, due to stricter collision constraints. The decline in performance becomes more significant for shorter measurement range. This means that the path of the main robot was likely blocked by the observation robots in the case with 4 observation robots.

C. Discussion on the Design Guideline

When we develop the actual hardware of robotic application, we will face various kinds of tradeoffs. In this paper, we focus on achieving design guidelines for actual applications, as those aforementioned. From the results shown in Fig. 7, we can find an adequate number of observation robots and sensors that provide suitable measurement range under the given disturbance level. If we can use a long range sensor such as laser, the multi-robot system of 3 observation robots is the best solution against the high level (50%) of disturbance. Additionally, if we can assume the lower levels of disturbance, 2 observation robots would be the best. If the measurement range is from 10m to 15m, the best solution is 2 observation robots, assuming 50% of disturbances. If we can use only short range sensors like as ultra-sonic, whose range is

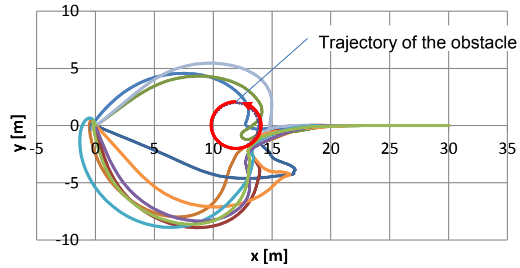

(a) Number of observation robots: 0

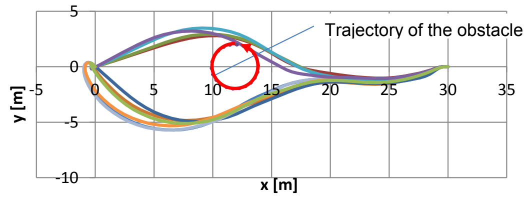

(b) Number of observation robots: 1

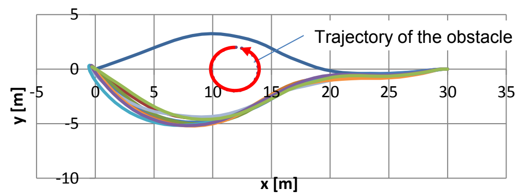

(c) Number of observation robots: 2

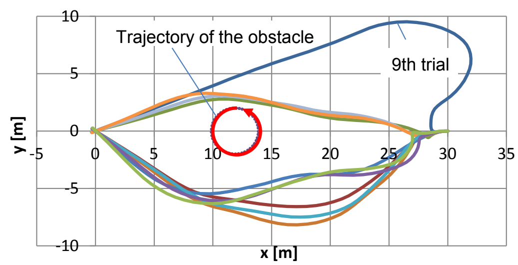

(d) Number of observation robots: 3

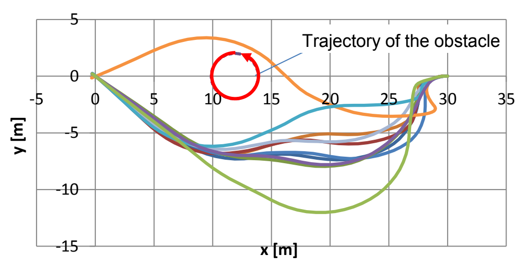

(e) Number of observation robots: 4

Figure 6. Trajectories of the main robot
(Disturbance level = 0%, Measurement range = 30 m)

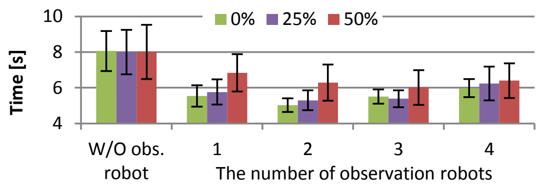

(a) Measurement range = 30 m

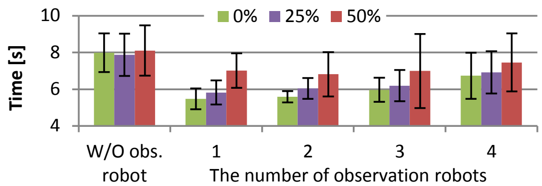

(b) Measurement range = 15 m

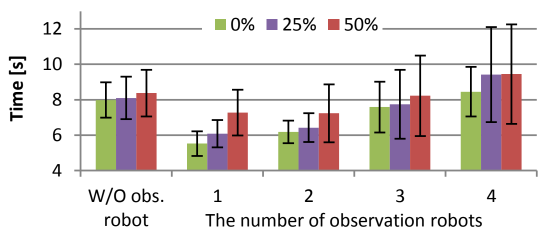

(c) Measurement range = 10 m

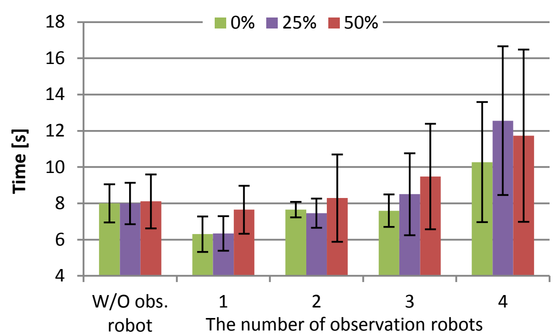

(d) Measurement range = 5 m

Figure 7. Average time taken to move to the goal

around 5m, only one observation robot is enough and too many observation robots will decrease the performance.

The aforementioned design guidelines depend on simulation conditions. For example, in this paper, the observation robots are controlled within 2D space. However, if they can move in 3D space, those negative impacts would be decreased. By improving the simulation models, our approach can achieve design guidelines for the actual applications.

IV. Conclusion

In this paper, we propose a new multi-robot control system that works in dynamic and uncertain environments. The proposed system uses multiple robots to decrease the amount of uncertainty in the environment and achieve high performance. Simulation results under various conditions on the disturbance level and the measurement range have clarified effects of the observation robots. The observation robots play a positive role in enhancing the capabilities of the main robots in order to avoid obstacles and arrive at the target points in shorter times. By increasing the number of the observation

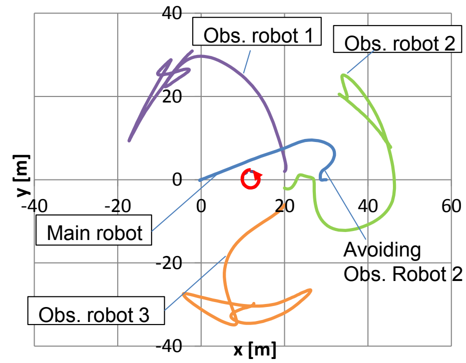

Figure 8. Trajectories of all robots (9th trial in Fig 6(d))

robots, the proposed system has shown its robustness against disturbances in sensing and communication. However, too many observation robots undermine performance by creating obstacles for the main robot. We find that the system with 2 or 3 observation robots achieves the best performance in almost all cases.

The simulation results in this paper suggest an optimal number of the observation robots as well as providing design guidelines for sensors and networks of the proposed system. Future work includes detailed modeling of disturbances in actual networks and sensors in order to evaluate performance of the proposed system in specific applications. Even though this paper addresses only one obstacle, this framework can be extended to track multiple objects using estimation methods such as JPDAF [11].

References

[1] D. Q. Mayne, M.M. Seron, and S.V. Rakovic, “Robust model predictive control of constrained linear systems with bounded disturbances,” *Automatica*, vol. 41, 2005, pp. 219-225.

[2] F. Oldewurtel, A. Parisio, C. N. Jones, M. Morari, D. Gyalistras, M. Gwerder, V. Stauch, B. Lehmann, and K. Wirth, “Energy efficient building climate control using Stochastic Model Predictive Control and weather predictions,” in *Proc. ACC*, Baltimore, 2010, pp. 5100-5105.

[3] G. M. Hoffmann and C. J. Tomlin. “Mobile sensor network control using mutual information methods and particle filters,” *IEEE Trans. Automatic Control*, vol. 55, No. 1, Jan 2010.

[4] B. Charrow, V. Kumar, N. Michael, “Approximate representations for multi-robot control policies that maximize mutual information,” *Autonomous Robots*, vol. 37, Issue 4, 383-400, 2014.

[5] S. Emoto, I. Akkaya, E. A. Lee. “Information seeking and model predictive control of a cooperative robot swarm,” in *Proc. SWARM 2015*, Kyoto, Oct 2015.

[6] P. D. Christofides, R. Scattolini, D. Munoz de la Pena, and J. Liu, “Distributed model predictive control: A tutorial review and future research directions,” *Computers and Chemical Engineering*, vol. 51, 2013, pp. 21– 41.

[7] S. Boyd and L. Vandenberghe, “Convex optimization,” *Cambridge University Press*, 2004.

[8] C. Ptolemaeus, editor. “System Design, Modeling, and Simulation using Ptolemy II”, Ptolemy.org, 2014.

[9] I. Akkaya, P. Derler, S. Emoto, E. A. Lee, “Systems engineering for industrial cyber-physical systems using aspects,” *Proceedings of the IEEE, 2016*, to be published.

[10] I. Akkaya, S. Emoto, E. A. Lee, “PILOT: An actor-oriented learning and optimization toolkit for robotic swarm applications”, presented at International Workshop on Robotic Sensor Networks, 2015.

[11] C. Rasmussen and G. D. Hager, “Probabilistic data association methods for tracking complex visual objects,” *IEEE Trans. Pattern Analysis and Machine Intelligence*, vol. 23, No. 6, 2001.